

1      **The “Notch” in Unstable Layers and the Stability Minimum in the Tropics**

2

3                    Marvin A. Geller,<sup>a</sup> Ling Wang,<sup>b</sup>

4                   <sup>a</sup> *Stony Brook University, Stony Brook, New York*

5                   <sup>b</sup> *GATS, Boulder, Colorado*

6

7                   *Corresponding author:* Marvin A. Geller, marvin.geller@stonybrook.edu

8

9

## ABSTRACT

10 In a previous paper, we identified a “notch” in unstable layers at Koror (7.3 °N, 134.5 °E),  
11 where there was a relative deficiency in thin unstable layers and a corresponding relative  
12 excess in thicker layers, at altitudes centered at 12 km. We hypothesized that this feature was  
13 associated with the previously identified stability minimum in the tropics at that same altitude.  
14 In this paper, we extend our studies of this “notch” and its association with the tropical stability  
15 minimum by examining other stations in the deep tropics and also some stations at higher  
16 latitudes within the tropics. We find that this “notch” feature is found at all the other radiosonde  
17 stations in the deep tropics that we examined. We also find that the annual variations in  
18 unstable layer occurrences at stations at higher latitudes within the tropics show variations  
19 consistent with our hypothesis that this “notch” is associated with the region of minimum  
20 stability in the tropics at altitudes centered around 12 km, in that the annual variation in this  
21 “notch” feature is consistent with the annual variation of minimum stability in this region. Two  
22 factors contribute to the “notch” feature. One is that the data quality control procedure of the  
23 analysis rejects many thin layers due to the small trend-to-noise ratio in the region of minimum  
24 stability. The other is that the cloud-top outflow, which was previously identified with the  
25 stability minimum, advects thicker unstable layers throughout the deep tropics at the altitudes  
26 of the “notch.”

27

28

## SIGNIFICANCE STATEMENT

29 Previous papers have separately identified a stability minimum in the tropics and a “notch”  
30 feature in the thicknesses of unstable atmospheric layers where there are less thin unstable  
31 layers and a corresponding excess of thicker unstable layers, both at altitudes around 12 km.  
32 We previously hypothesized that these two features were associated with one another. In this  
33 paper, we examine this “notch” feature and the minimum in atmospheric stability at both deep  
34 tropical radiosonde stations and stations located at higher latitudes in the tropics, and we find  
35 that the annual variation of this “notch” feature is consistent with the latitudinal migration of  
36 the latitudes of the stability minimum. Turbulence associated with this “notch” feature might be  
37 significant for aircraft operations.

38

39

40 **1. Introduction**

41 Geller et al. (2021) reported finding a “notch” feature at Koror (7.3 °N, 134.5 °E), where  
42 there was a relative deficiency in thin unstable layers at altitudes centered at about 12 km,  
43 accompanied by a relative excess in thicker unstable layers at those altitudes. They  
44 hypothesized that this “notch” feature was associated with the region of minimum stability  
45 found by Grise et al. (2010). Gettelman and Forster (2002) and Fueglistaler et al. (2009) had  
46 earlier noted this climatological feature, and they associated it with the region of convective  
47 cloud outflow. Geller et al. (2024) have reexamined the atmospheric unstable layer results of  
48 Geller et al. (2021) when the processed US High Vertical-Resolution Radiosonde Data  
49 (HVRD) were analyzed instead of the raw data used in Geller et al. (2021), and they noted  
50 two factors that contributed to this “notch” feature. With respect to the deficiency of thin  
51 unstable layers, Geller et al. (2024) suggested that the data quality methodology of Wilson et  
52 al. (2010) and Wilson et al. (2011) played a major role in contributing to this deficiency since  
53 at the stability minimum, the trend-to-noise ratio (tnr) in the potential temperature profiles is  
54 small, there will be a greater rejection of the thinner overturns. They also noted the advection  
55 of cloud-top turbulence would account for the excess of thicker unstable layers in the “notch”  
56 region, and the larger eddies of this cloud-top turbulence provide turbulent mixing of the  
57 thinner unstable layer environment, forming thicker unstable layers.

58 Given the results of Geller et al. (2021) and Geller et al. (2024), we expect the following.

59 

1. We expect that the “notch” feature, seen at Koror, is present at all radiosonde stations in  
60 the deep tropics.
2. We expect that the annual variations of the “notch” feature at higher latitude tropical  
62 radiosonde stations will be consistent with the annual migration of the latitudes of this  
63 stability minimum at altitudes around 12 km.

64

65 To confirm these expectations, we analyze the distribution of atmospheric unstable layers  
66 of various thicknesses using temperature data from the 1-second US HVRD. This is the same  
67 dataset that has been analyzed for turbulence by Ko et al. (2019) and for the climatology of  
68 unstable layers by Geller et al. (2021). Details of this dataset were given in both those papers.  
69 Geller et al. (2021) used the raw HVRD for their analysis, while Ko et al. (2019) used the  
70 processed HVRD in their analysis.

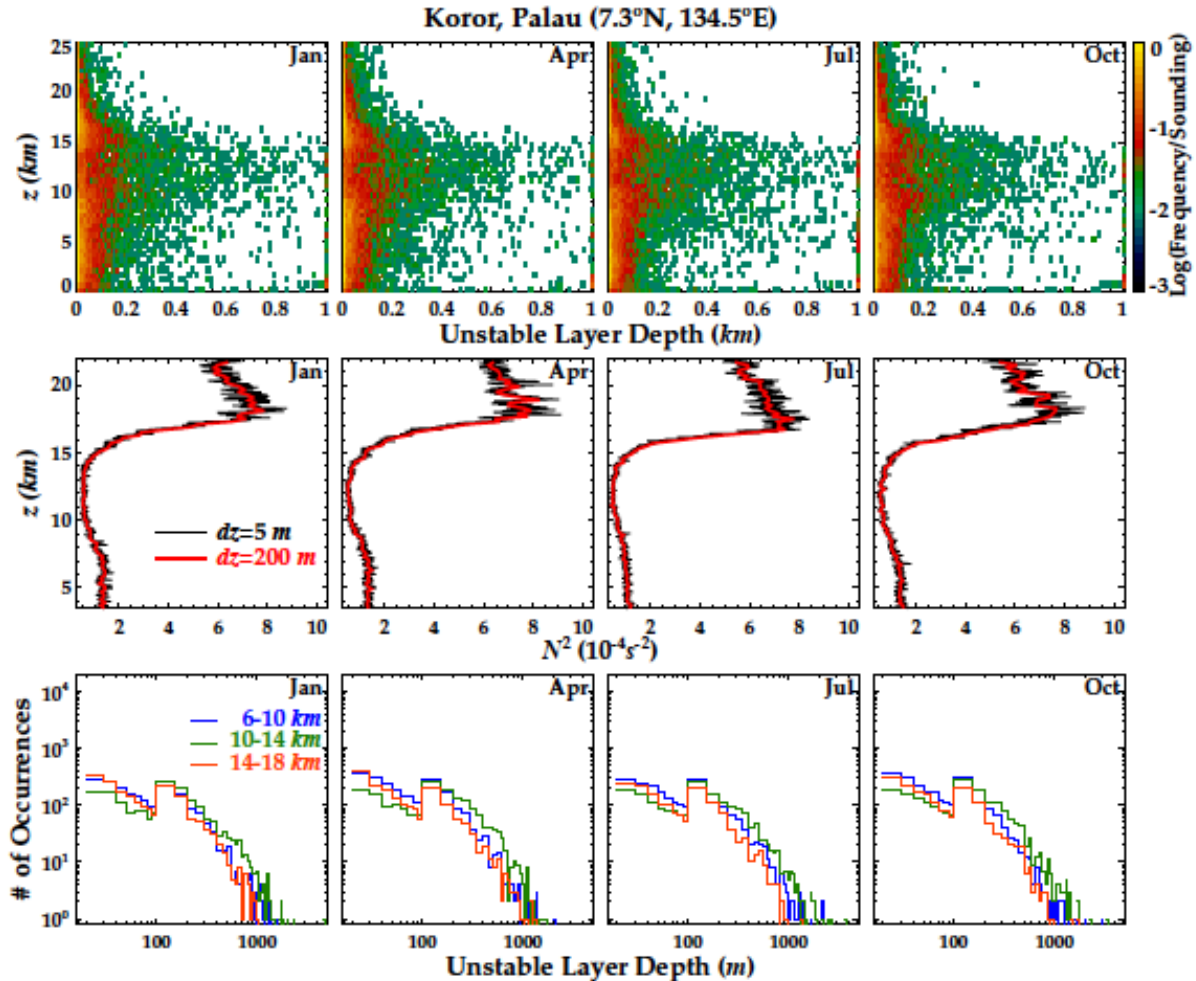
71 The processed HVRD have been radiation corrected, i.e., the temperature data have been  
72 adjusted to take into account how the solar radiation falling on the radiosonde temperature  
73 sensor results in temperature readings that differ from the actual atmospheric temperatures. The  
74 processed HVRD have also been smoothed, the details of this smoothing being proprietary to  
75 the radiosonde manufacturer. Given this, Wang and Geller (2024) have tried to understand  
76 aspects of this smoothing by looking at temperature fluctuations of various vertical scales in  
77 raw and processed HVRD. They found that there were spurious temperature fluctuations at  
78 small vertical scales during daytime in both the raw and processed data, and that those spurious  
79 temperature fluctuations were greatly diminished, but not eliminated, in the processed data  
80 relative to those in the raw data.

81 Geller et al. (2024) discussed how the use of the raw HVRD affected the conclusions  
82 about the atmospheric unstable layer climatology in Geller et al. (2021). Specific to the present  
83 paper, Geller et al. (2024) concluded that the “notch” feature at Koror noted in Geller et al.  
84 (2021) was present in both the raw and processed HVRD, but that this “notch” feature at  
85 Koror was more obvious when the daytime raw HVRD were analyzed than when the  
86 processed daytime data were analyzed, and that this “notch” feature looked very similar at  
87 Koror in both the nighttime raw and processed data. They noted that there was a smaller  
88 deficiency in thin unstable layers in this notch region when the processed data were used than  
89 when the raw data were used. They attributed much of the smaller deficiency in thin unstable  
90 layers in this “notch” region to the data quality control procedures of Wilson et al. (2010) and  
91 Wilson et al. (2011), which leads to the rejection of many of the thin layers in this region due to  
92 the small tnr in the region of the stability minimum.

## 93 **2. The “notch” in the deep tropics**

94 Figure 1 shows the distribution of the  $\log_{10}$  frequency of occurrence per sounding of unstable  
95 layers of various thicknesses as a function of altitude at Koror, Palau ( $7.3^{\circ}\text{N}$ ,  $134.5^{\circ}\text{E}$ ), as  
96 computed using the processed data at 1200 UTC for the months January, April, July, and  
97 October using all the data that were available to us at the time, namely, 2012-2018 for January,  
98 2011-2018 for April and July, and 2011-2017 for October. The methodology to derive the  
99 unstable layer statistics from the 1-second US HVRD follows closely Geller et al. (2021)  
100 except that the processed data are analyzed here. Basically, we perform Thorpe analysis  
101 (Thorpe, 1977), which has been adapted for the analysis of atmospheric turbulence.  
102 Specifically, we follow Wilson et al. (2010) and Wilson et al. (2011) to detect turbulence

103 overturning events that can be distinguished from measurement noise. We also apply the  
 104 techniques of Wilson et al. (2013) to account for the destabilizing effect of water vapor, which  
 105 is particularly important in the troposphere.



106  
 107 Figure 1. Top Row – Distribution of the thicknesses of unstable layers at Koror in January, April, July,  
 108 and October calculated from processed HVRD at 1200 UTC. Middle Row – Monthly mean  
 109  $N^2$  profiles for Koror for January, April, July, and October. Black curves are results using the  
 110 native 5 m resolution data, and the red curves show the results using 300 m resolution  
 111 smoothed data. Bottom Row – Histograms for the thicknesses of unstable layers for the  
 112 altitude regions 6-10 km (blue), 10-14 km (green), and 14-18 km (red).

113  
 114 We show the 1200 UTC results since Wang and Geller (2024) have shown that the nighttime  
 115 HVRD are less “noisy” than are the daytime data. Furthermore, Geller and Wang (2024) have  
 116 shown that the 1200 UTC (nighttime) view of the “notch” at Koror using the raw HVRD is  
 117 very similar to that calculated using the 1200 UTC processed HVRD. Figure 1 also shows the  
 118 corresponding monthly mean  $N^2$  profiles for those same months, and also “notch” histograms,

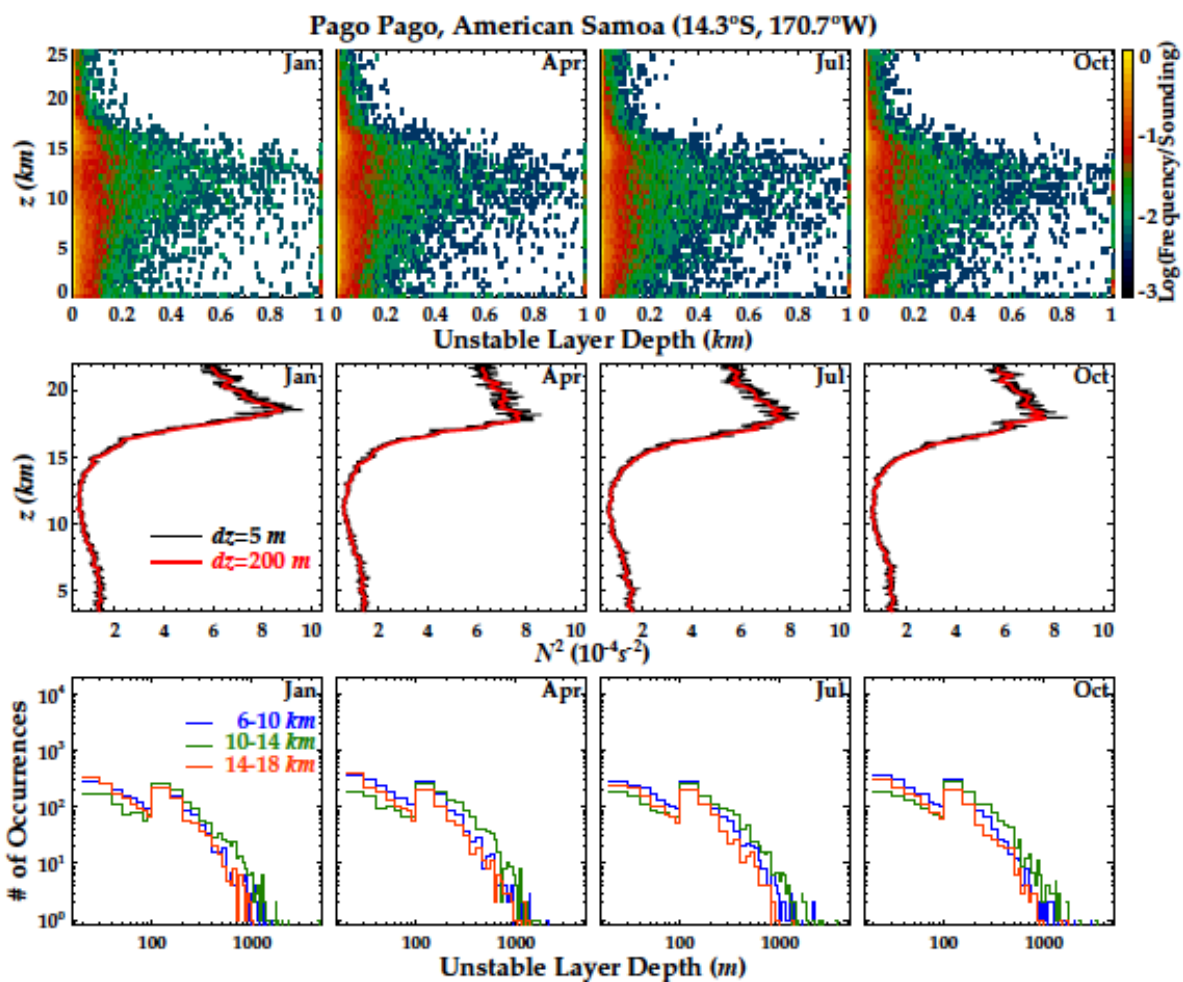
similar to what was shown in figure 11 in Geller et al. (2021) for the same months. Note that there is a stability minimum at altitudes centered at about 12 km in the  $N^2$  profiles in all months, with this minimum being slightly deeper in July. This is consistent with the stability minimum results of Grise et al. (2010). Examining the histograms, we see that there are clear deficiencies in the thinnest layers and enhancements in thicker unstable layers for all months in the 10-14 km region, the “notch” region, relative to the 4 km thick regions directly above and below the “notch” region. Also, note that similar results are shown in the supplementary figures for the other deep tropical stations we have analyzed – Ponape, Micronesia ( $7.0^{\circ}\text{N}$ ,  $158.2^{\circ}\text{E}$ ), Chuuk, Micronesia ( $7.5^{\circ}\text{N}$ ,  $151.8^{\circ}\text{E}$ ), Majuro, Marshall Islands ( $7.1^{\circ}\text{N}$ ,  $171.3^{\circ}\text{E}$ ), and Yap, Micronesia ( $9.5^{\circ}\text{N}$ ,  $138.1^{\circ}\text{E}$ ); that is to say, a clear “notch” is seen in all months, as is the clear minimum in  $N^2$  at altitudes centered at about 12 km, and also enhancements in the thicker unstable layers in the 10-14 km region of the “notch” relative to the 6-10 and 14-18 km altitude regions.

Having seen that the existence of this “notch” in unstable layers and the stability minimum at altitudes centered around 12 km are present in all the deep tropical stations that we have examined, we now look at the annual behavior of this “notch” and the stability minimum at higher latitudes in the tropics.

### 3. The “notch” at higher latitude tropical stations

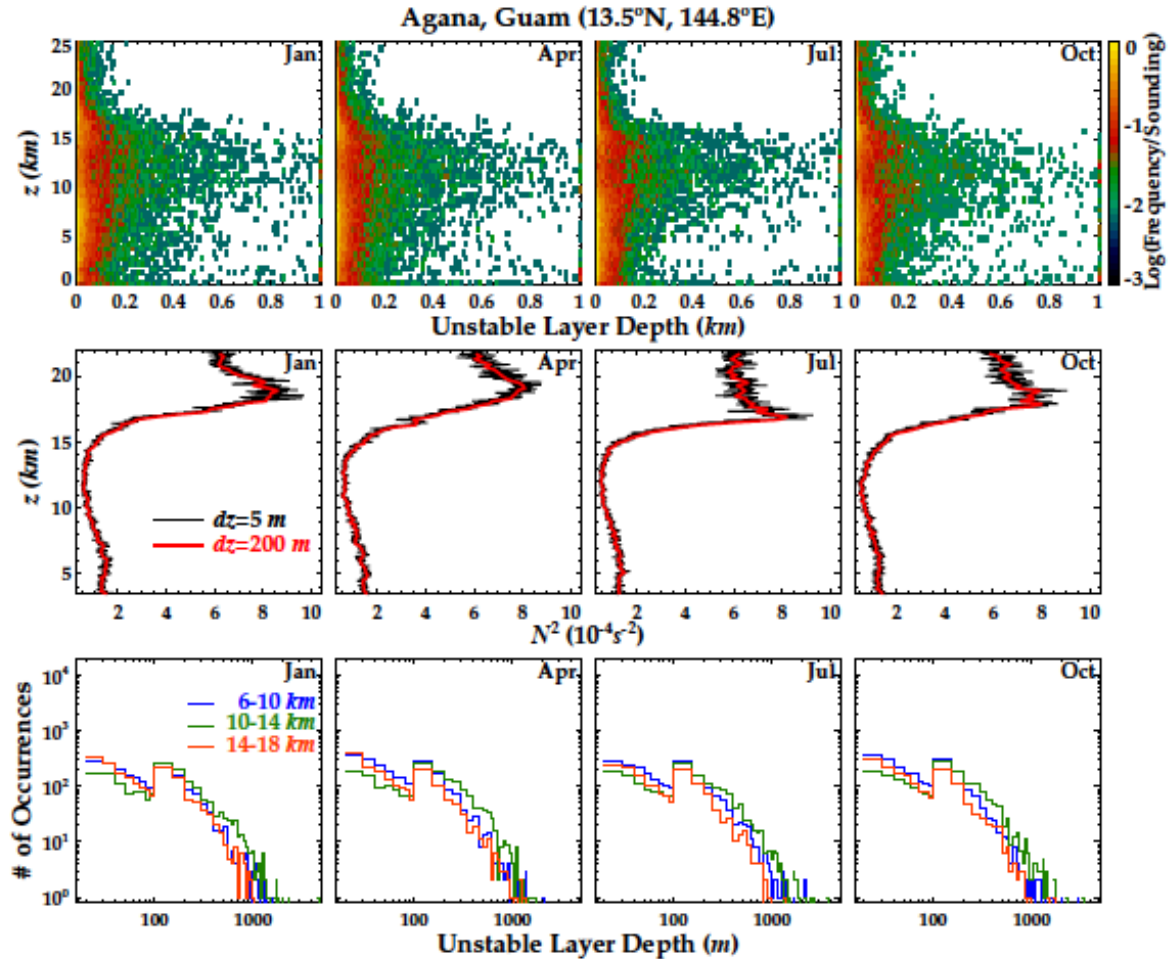
Looking at figure 3 of Grise et al. (2010), we see that the region of deepest stability minimum extends from about  $18^{\circ}\text{S}$  to about  $16^{\circ}\text{N}$  in the DJF season, extends from about  $15^{\circ}\text{S}$  to about  $15^{\circ}\text{N}$  in the MAM season, extends from about  $16^{\circ}\text{S}$  to about  $20^{\circ}\text{N}$  in the JJA season, and extends from about  $16^{\circ}\text{S}$  to about  $19^{\circ}\text{N}$  in the SON season. Thus, the southern edge of this region of the deepest stability minimum migrates by about  $3^{\circ}$  while the northern edge of this region of stability minimum migrates by about  $5^{\circ}$  throughout the year. Given this, we examine tropical stations at the northern and southern edges of the deep tropics to see if the “notch” feature evolution throughout the year is consistent with the seasonal migration of the stability minimum. The stations we examine are Pago Pago, American Samoa ( $14.3^{\circ}\text{S}$ ,  $170.7^{\circ}\text{W}$ ), Agana, Guam ( $13.5^{\circ}\text{N}$ ,  $144.8^{\circ}\text{E}$ ), and San Juan, Puerto Rico ( $18.4^{\circ}\text{N}$ ,  $66.0^{\circ}\text{W}$ ). Figure 2 shows results at Pago Pago. At Pago Pago, we see that there is a “notch” feature, i. e., a deficiency of thin unstable layers at altitudes centered about 12 km, and there are also many thicker unstable layers at altitudes centered at about 12 km in all four months. Looking at the stability profiles next, we see the deep minima in  $N^2$  in all four months at about 12 km altitude,

151 with the deepest minimum in January. The histograms for Pago Pago are consistent with this in  
 152 that the there are excesses in thicker unstable layers in all four months, but the shape of the  
 153 histograms in January and April most resemble those in the deep tropics. This is consistent with  
 154 Figure 4 in Grise et al. (2010), in that Pago Pago is within the region of minimum stability in  
 155 all four months. The “notch” feature at Pago Pago is not as marked as at Koror though in terms  
 156 of the deficiency of thin unstable layers, the excess in thicker layers, and the depth of the  
 157 minimum stability at an altitude of about 12 km. This is consistent with Pago Pago being near  
 158 the edge of the minimum stability region, where the stability minimum is not as marked as in  
 159 the deep tropics.



160  
 161 Figure 2. Same as figure 1, but for Pago Pago. The data used for Pago Pago in Started in February of  
 162 2011 and ended in August of 2019.

163 Results for Agana are shown in figure 3. At Agana, we see a more prominent “notch”  
 164 feature in than at Pago Pago even though Agana is only 0.8 ° closer to the Equator, but in the



165

166 Figure 3: Same as figures 1 and 2, but at Agana. The data used for Agana began in April of 2011 and  
 167 ended in August of 2019.

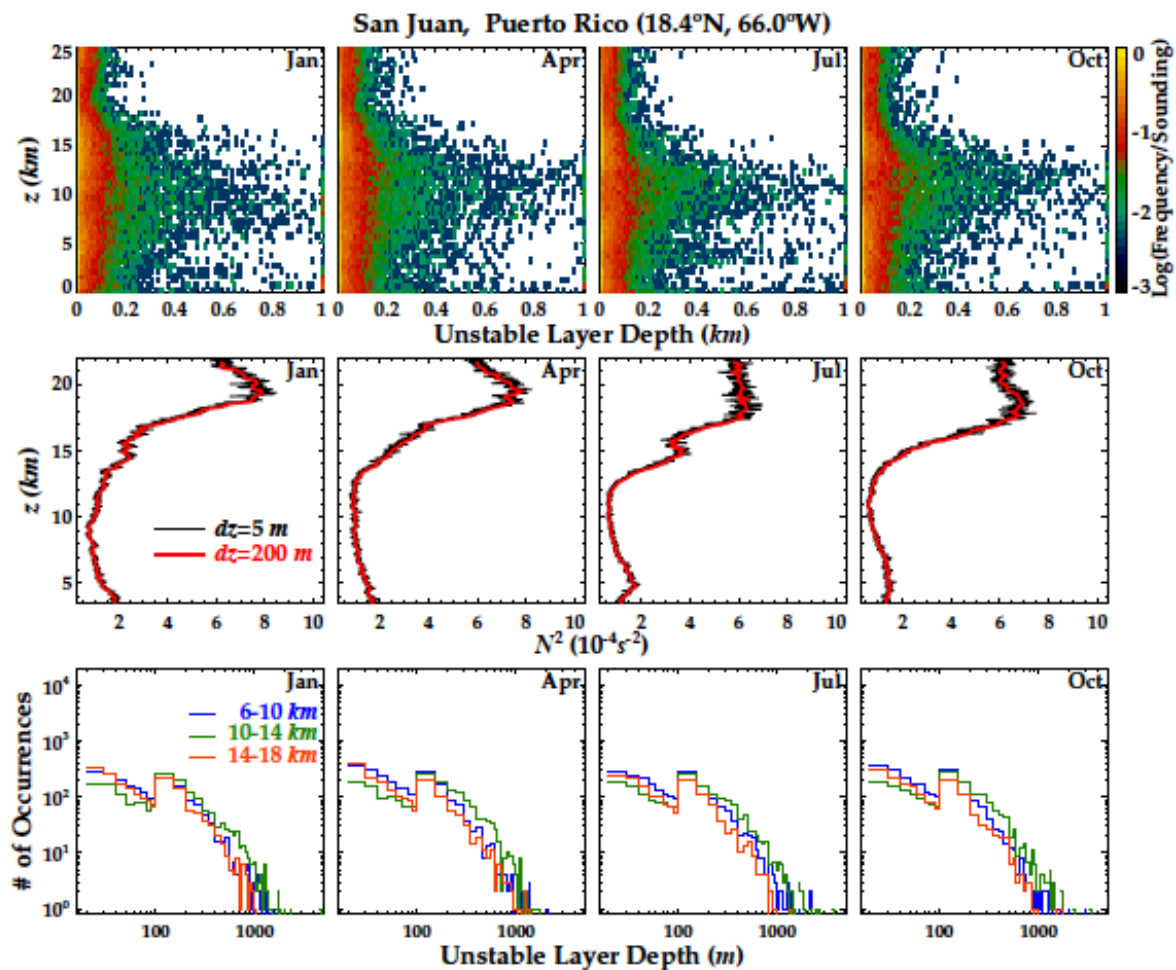
168 Northern Hemisphere. This is consistent with the Northern Hemisphere bias in the latitudes of  
 169 minimum stability, which was noted earlier in this section.<sup>1</sup> We also see deeper stability  
 170 minima at Agana than at Pago Pago, particularly in July and October. In addition, the

---

<sup>1</sup> Note that there is a much larger Northern Hemisphere bias in the annual migration of the ICTZ (Inter-Tropical Convergence Zone) than in the annual migration of the stratospheric stability minimum.

171 histograms at Agana show greater excesses in thick unstable layers than were seen at Pago  
172 Pago.

173 Next, we look at the results at San Juan in figure 4. This is the highest latitude station at  
174 which the “notch” feature is examined in this paper. At San Juan, we do not see a clear “notch,”  
175 where there is a marked deficiency in thin unstable layers such as was seen at the lower latitude  
176 stations, but we do see a clear excess of thick unstable layers that is centered at altitudes near  
177 12 km, and most peaked, in October. Looking at the stability profiles, this “notch” picture  
178 seems quite consistent with the stability where the stability minimum in October is highest and



179  
180 Figure 4. Same as figures 1, 2, and 3, but for San Juan, Puerto Rico. The data used for San Juan started  
181 in March of 2010 and ended in August of 2019.  
182 deepest. The stability minima are most marked in July and October. In January, the minimum  
183 stability is at much lower altitudes, centered at about 9 km, and is not as deep as in July and  
184 October. In April, again the stability minimum is not as deep as in July and October and is

185 broader in altitude. This is consistent with San Juan being outside the stability minimum  
186 latitude range during January and April. The histograms show excesses in thick unstable layers  
187 in all four months, but these excesses are not as marked as in the deep tropics. This picture is  
188 broadly consistent with figure 4 of Grise et al. (2010).

#### 189 **4. Summary and Conclusions**

190 In a previous paper, Geller et al. (2021) identified a “notch” feature at Koror (7.3  $^{\circ}$ N, 134.5  
191  $^{\circ}$ E), where this “notch” feature was characterized by a relative deficiency in thin atmospheric  
192 layers at altitudes centered at about 12 km, and a relative excess of thick atmospheric unstable  
193 layers at those altitudes. We also hypothesized that this “notch” feature was associated with the  
194 stability minimum in the tropics that was identified by Grise et al. (2010). This paper further  
195 investigates these topics by analyzing the unstable layer distribution  
196 at four additional stations in the deep tropics, within 10  $^{\circ}$  of the Equator, where US HVRD are  
197 available. Those stations vary in their longitude from about 171 to 138  $^{\circ}$ E. We found “notch”  
198 features very similar to what we found at Koror at all those stations.

199 To test our hypothesis that this “notch” feature is associated with the stability minimum in  
200 the tropics that was identified by Grise et al. (2010), we analyzed the US HVRD at stations  
201 that were located slightly poleward of the deep tropics: Agana, Guam at 13.5  $^{\circ}$ N and Pago  
202 Pago, American Samoa at 14.3  $^{\circ}$ N. We also examined one US HVRD station located further  
203 poleward, San Juan, Puerto Rico at 18.4  $^{\circ}$ N. We then examined whether the seasonal variations  
204 of this “notch” feature were consistent with the migration of the stability minimum, identified  
205 by Grise et al. (2010), annually into the summer hemisphere. We found that the annual  
206 variation of the “notch” feature at those stations was broadly consistent with the annual  
207 migration of the stability minimum feature. To identify the annual migration of the stability  
208 minimum, we examined the stability profiles at those stations for the same months when the  
209 “notch” was examined. We also looked at the histograms for the thicknesses of atmospheric  
210 unstable layers. The annual variations of those histograms were consistent with the overall  
211 picture of the “notch” region and with the stability minimum in the tropics and its annual  
212 migration in latitude.

213 Grise et al. (2010) indicated that the deep tropical stability minimum region centered at  
214 about 12 km altitude had been noted in previous papers by Gettelman and Forster (2002) and  
215 Fueglistaler et al. (2009), and that those previous authors associated this stability minimum

216 with convective cloud outflow. This study suggests that the “notch” feature might be the  
217 signature of large eddies associated with turbulence at convective cloud tops being advected  
218 throughout the tropics at altitudes around 12 km, resulting in the advection of low stability air  
219 and the mixing of small unstable regions, resulting in less thin layers and more thick unstable  
220 layers at those altitudes. There is another important factor accounting for the depletion of thin  
221 unstable layers in the “notch” region, and that is the elimination of many of the thin layers  
222 through the use of the Wilson et al. (2010) and Wilson et al. (2011) methodology. In this  
223 methodology, small overturns are rejected as likely being a result of “noise” in the sounding.  
224 The identification procedure uses the tnr (trend-to-noise ratio) as a criterion, and in the region  
225 of the stability minimum the tnr is smallest, so there is greatest rejection of thin overturns.

226 We do not know how many of the soundings analyzed in this paper were taken in  
227 convective cloud regions and how many were in cloud-free regions. In principle, we can use  
228 the humidity measurements from the soundings to see if a sounding traveled through a cloud  
229 region, but humidity measurements in the upper troposphere at altitudes near 12 km are  
230 unreliable. Satellite measurements could be used to look if the various soundings traveled  
231 through clouds, but that is beyond the scope of this paper. Of course, one expects turbulence  
232 inside clouds, but the fact that the excess in thick unstable layers is confined to altitudes around  
233 12 km suggests that we are “seeing” unstable layers associated with the advection of turbulent  
234 eddies from cloud-top turbulence.

235 It should be noted that 12 km corresponds to an altitude of 39,370 feet, which is not an  
236 uncommon altitude for aircraft flying long distance routes crossing the Equator. It would be  
237 interesting to see what, if any, effect this change in unstable layer thicknesses in the “notch”  
238 region might have on aviation turbulence.

239

240

241 *Acknowledgments.*

242 This research was supported by National Science Foundation Grants AGS-2032678 and  
243 AGS-2129221. We acknowledge the Fine-Scale Atmospheric Processes and Structures  
244 (FISAPS) activity of the Atmospheric Processes And their Role in Climate (APARC) project of  
245 the World Climate Research Programme (WCRP) in encouraging this research.

246

247 *Data Availability Statement.*

248 Radiosonde data analyzed in this study were obtained from the U.S. National Oceanic and  
249 Atmospheric Administration National Centers for Environmental  
250 Information: <ftp://ftp.ncdc.noaa.gov/pub/data/ua/>.

251

## 252 REFERENCES

253 Fueglistaler, S., A. E. Dessler, T. J. Dunkerton, I. Folkins, Q. Fu, and P. W. Mote, 2009: The  
254 tropical tropopause. *Rev. Geophys.*, **47**, RG1004,  
255 <https://doi.org/10.1029/2008RG000267>.

256 Geller, M. A., P. T. Love, and L. Wang, 2021: Climatology of Unstable Layers in the  
257 Troposphere and Lower Stratosphere: Some Early Results, *Mon. Wea. Rev.*, **149**, 233-  
258 245, <https://doi.org/10.1175/MWR-D-20-0276.1>.

259 Geller, M. A., L. Wang, and P. T. Love, 2024: Climatology of Atmospheric Unstable Layers  
260 Revisited A Corrigendum, Submitted to *Mon. Wea. Rev.*

261 Gettelman, A., and F. Forster, 2002: A climatology of the tropical tropopause layer.  
262 *J. Meteor. Soc. Japan*, **80**, 911–924, <https://doi.org/10.2151/jmsj.80.911>.

263 Grise, K. M., D. W. J. Thompson, and T. Birner, 2010: A global survey of static stability in the  
264 stratosphere and upper troposphere. *J. Climate*, **23**, 2275–2292,  
265 <https://doi.org/10.1175/2009JCLI3369.1>.

266 Ko, H.-V., H.-Y. Chun, R. Wilson, and M. A. Geller, 2019: Characteristics of turbulence in the  
267 free atmosphere retrieved from high vertical-resolution radiosonde data in U.S., *J.*  
268 *Geophys. Res. Atmos.*, **124**, 7553–7579, <https://doi.org/10.1029/2019JD030287>.

269 Thorpe, S. A. (1977). Turbulence and mixing in a Scottish Loch. Philosophical Transactions of  
270 the Royal Society A Mathematical, Physical and Engineering Sciences, 286, 125–181.  
271 doi.org/10.1098/rsta.1977.0112.

272 Wang, L., and M. A. Geller, 2024: Temperature Fluctuations of Different Vertical Scales in  
273 Raw and Processed US High Vertical-Resolution Radiosonde Data, Submitted to *J.*  
274 *Atmos. and Ocean Tech.*

275 Wilson, R., Dalaudier, F., and Luce, H. (2011). Can one detect small-scale turbulence from  
276 standard meteorological radiosondes? *Atmos. Meas. Tech.*, 4, 795-804,  
277 doi:10.5194/amt-4-795-2011.

278 Wilson, R., Luce, H., Dalaudier, F., & Lefrère, J. (2010). Turbulence patch identification in  
279 potential density or temperature profiles. *J. of Atmospheric and Oceanic Technology*,  
280 27(6), 977– 993. <https://doi.org/10.1175/2010JTECHA1357.1>. 34.

281 Wilson, R., H. Luce, H. Hashiguchi, M. Shiotani, and F. Dalaudier, 2013: On the effect of  
282 moisture on the detection of tropospheric turbulence from in situ measurements. *Atmos.*  
283 *Meas. Tech.*, 6, 697–702, doi:10.5194/amt-6-697-2013.

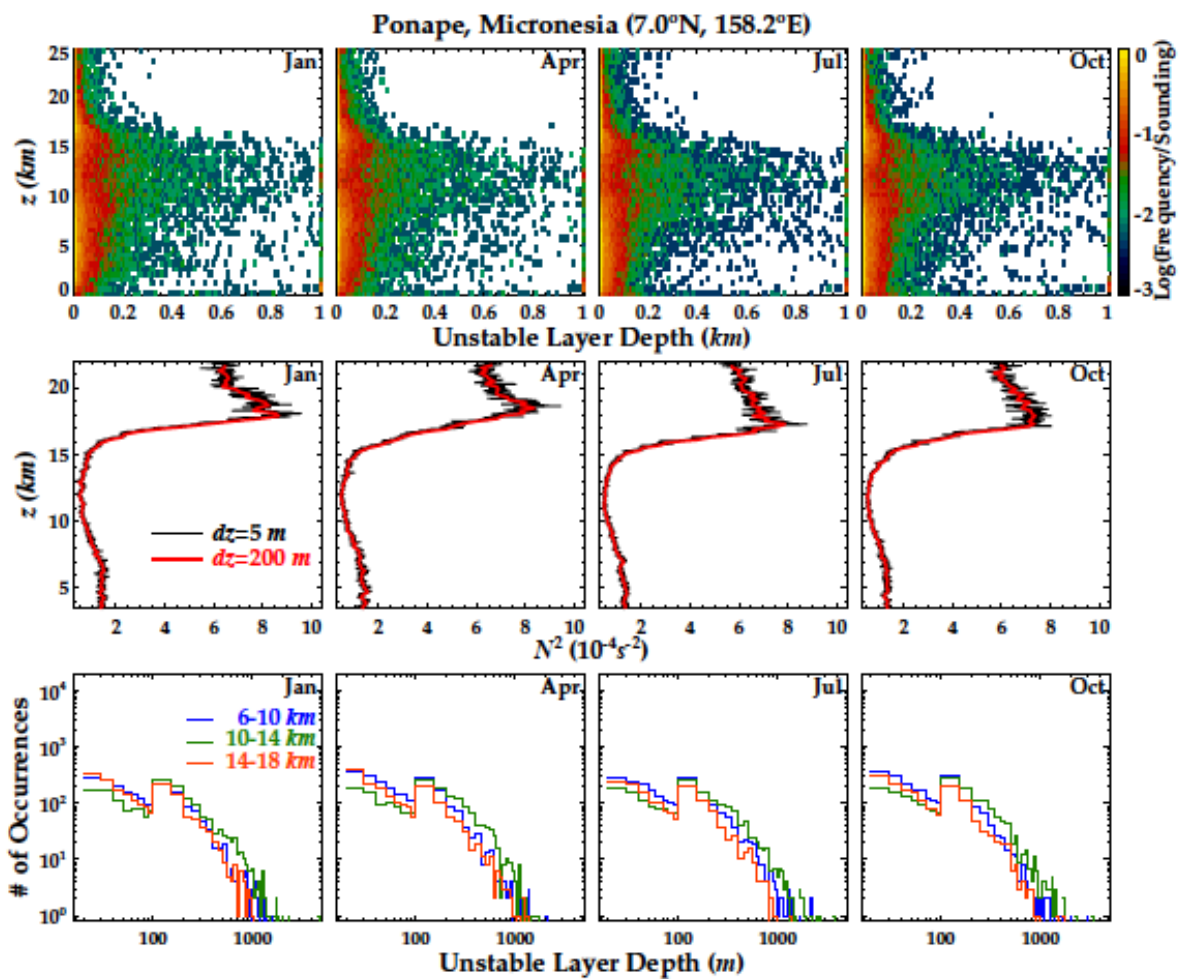
284

285

## Supplementary Figures

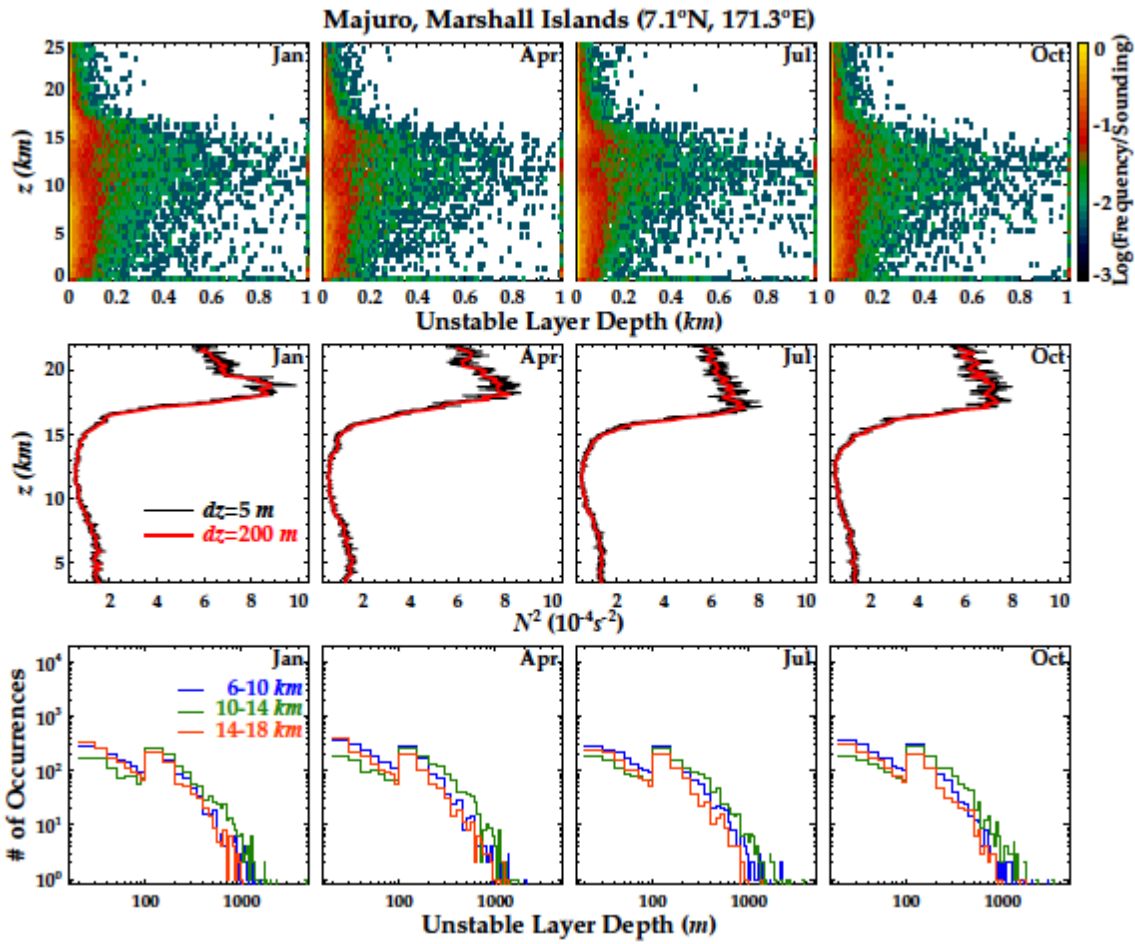
286

287 The following are figures, in the same format as figures 1, 2, 3, and 4, for the additional  
 288 stations in the deep tropics that we have analyzed: Ponape ( $7.0^{\circ}\text{N}$ ,  $158.2^{\circ}\text{E}$ ), Majuro ( $7.1^{\circ}\text{N}$ ,  
 289  $171.3^{\circ}\text{E}$ ), Chuuk ( $7.5^{\circ}\text{N}$ ,  $151.8^{\circ}\text{E}$ ), and Yap ( $9.5^{\circ}\text{N}$ ,  $138.0^{\circ}\text{E}$ ). Note that the nature of the  
 290 “notch” in unstable layers seen at altitudes centered at about 12 km, the stability profiles, and  
 291 the histograms look very similar to what is seen in figure 1 at Koror ( $7.3^{\circ}\text{N}$ ,  $134.5^{\circ}\text{E}$ ).



292

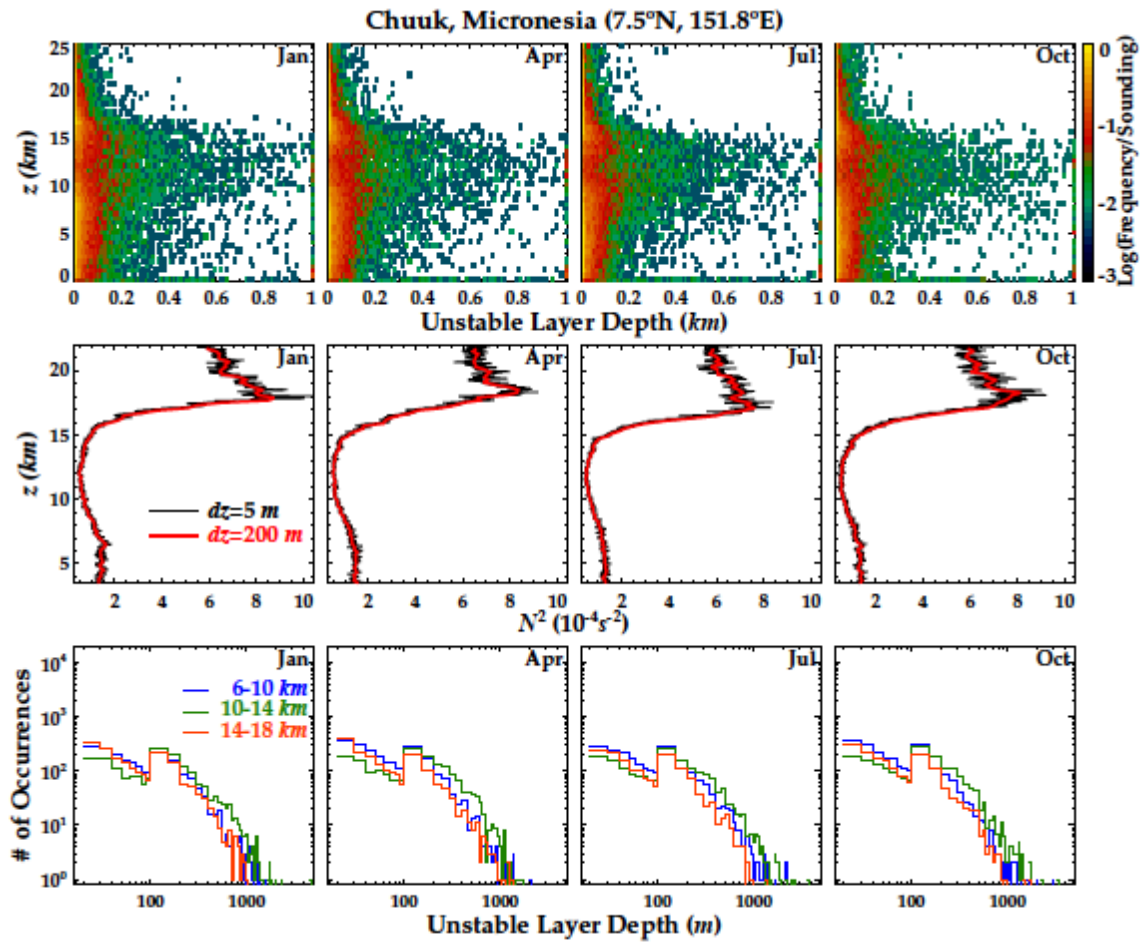
293 Figure S1. Top – Distribution of the thicknesses of unstable layers at Ponape in January, April, July, and  
 294 October calculated from processed HVRD at 1200 UTC. Middle – Monthly mean  $N^2$   
 295 profiles for Ponape for January, April, July, and October. Black curves are results using the  
 296 native 5 m data, and the red curves show the results using 300 m smoothed data. Bottom –  
 297 Histograms for the thicknesses of unstable regions for the altitude regions 6-10 km, 10-14 km  
 298 (the “notch” region, and 14-18 km. The data used for Ponape began in May of 2011 and  
 299 ended in August of 2019.



300

301 Figure S2. Same as figure S1, but for Majuro. The data used for Majuro began in May of 2011 and  
 302 ended in August of 2019.

303



304

305 Figure S3. Same as figures S1 and S2, but for Chuuk. The data used for Chuuk began in May of 2011  
 306 and ended in August of 2019.

